Electronic Supplementary Information†

A photofuel cell comprising titanium oxide and silver(I/0) photocatalysts for use of acidic water as a fuel

Yuta Ogura,[a] Seiji Okamoto,[a] Takaomi Itoi,[b] Yukiko Fujishima,[c,a] Yusuke Yoshida,[a] and Yasuo Izumi*[a]

[a] *Department of Chemistry, Graduate School of Science, Chiba University, Yayoi 1-33, Inage-ku, Chiba 263-8522, Japan., Fax: +81-43-290-2783; Tel: +81-43-290-3696; E-mail: yizumi@faculty.chiba-u.jp*

[b] *Department of Mechanical Engineering, Graduate School of Engineering, Chiba University, Yayoi 1-33, Inage-ku, Chiba 263-8522, Japan.*

[c] *Department of Chemistry, Faculty of Science, Tokyo University of Science, Kagurazaka 1-3, Shinjuku-ku, Tokyo 163-8601, Japan.*

Derivation of Equation 2. The kinetic model of photocurrents in the PFCs was formulated based on the principle as shown in Scheme 1. The equilibrium constants K_a and K_c were defined in the main text, for the separation of electrons and holes in anodic TiO_2 and cathodic Ag-TiO_2, respectively, which are irradiated by light. $[O_2]$, $[H^+]$, $[H_2O]$, $[Ti^{4+}]$, $[Ti^{3+}]$, $[O^{2-}]$, $[O^-]$, $[Ag^+]$, and $[Ag^0]$ were the concentrations of O_2, H^+, and H_2O in the electrolyte solution and the concentrations of Ti^{4+}, Ti^{3+}, O^{2-}, O^-, Ag^+, and Ag^0 in photocatalysts with a subscript "a" (anode) or "c" (cathode). $[O^-]$ denotes hole concentrations at VB of TiO_2 and $[Ti^{3+}]_a$ and $[Ag^0]_c$ denote electron concentrations at CB of TiO_2 and trapping sites of Ag nanoparticles, respectively.

$$K_a = \frac{\left[Ti^{3+}\right]_a \left[O^-\right]_a}{\left[Ti^{4+}\right]_a \left[O^{2-}\right]_a} \qquad \text{(S1)}$$

$$K_c = \frac{\left[Ag^0\right]_c \left[O^-\right]_c}{\left[Ag^+\right]_c \left[O^{2-}\right]_c} \quad \text{(S2)}$$

Nitrogen gas was bubbled through the acidic solution for TiO_2 to purge O_2. In a separate experiment, O_2 was recycled to irreversibly transfer to the gas phase of the anode compartment through an organic layer and then to the cathode compartment through small vent holes in the PCP film (Graphical abstract). The reaction rate at anode is formally proportional to the fourth power of $[O^-]_a$ as it is four-electron oxidation (Scheme 1).

$$r_{ox} = k_{ox} \left(\left[H_2O\right]_a\right)^2 \left(\left[O^-\right]_a\right)^4 \quad \text{(S3)}$$

For the equilibrium of O_2 photoreduction, forward and reverse reaction rates were formally proportional to the fourth powers of $[Ag^0]_c$ and $[O^-]_c$, respectively, because they were four-electron reactions (Scheme 1).

$$K_{red} = \frac{\left(\left[H_2O\right]_c\right)^2 \left(\left[O^-\right]_c\right)^4}{\left[O_2\right]_c \left(\left[H^+\right]_c\right)^4 \left(\left[Ag^0\right]_c\right)^4} \quad \text{(S4)}$$

The net electron flow rate (photocurrent) is the difference in the forward electron flow from TiO_2 to Ag-TiO_2 via the external circuit, and the reverse electron flow from TiO_2 to Ag-TiO_2 via the external circuit.

$$\text{Photocurrent } i = k\left[Ti^{3+}\right]_a \left[O^-\right]_c - k'\left[Ag^0\right]_c \left[O^-\right]_a$$

$$= k \frac{K_a' (k_{ox}')^{\frac{1}{4}} (K_c')^{\frac{1}{2}} (K_{red}')^{\frac{1}{8}}}{(r_{ox})^{\frac{1}{4}}} \left(\left[O_2\right]_c\right)^{\frac{1}{8}} \left(\left[H^+\right]_c\right)^{\frac{1}{2}} - k' \frac{(r_{ox})^{\frac{1}{4}} (K_c')^{\frac{1}{2}}}{(k_{ox}')^{\frac{1}{4}} (K_{red}')^{\frac{1}{8}}} \frac{1}{\left(\left[O_2\right]_c\right)^{\frac{1}{8}} \left(\left[H^+\right]_c\right)^{\frac{1}{2}}} \quad \text{(2)}$$

Here, the equilibrium constants with the prime symbol are as follows: $K_a' = K_a \left[Ti^{4+}\right]_a \left[O^{2-}\right]_a$, $K_c' = K_c \left[Ag^+\right]_c \left[O^{2-}\right]_c$, $K_{red}' = K_{red} / \left(\left[H_2O\right]_c\right)^2$, and $k_{ox}' = k_{ox} \left(\left[H_2O\right]_a\right)^2$.

The solubility of O_2 in water is insensitive to the pH value: 4.063 and 4.060 mg per 100 mL of water (1.27 mmol L^{-1}) at pHs of 2.0 and 4.0, respectively. The H^+ concentrations (10 mmol L^{-1}) were greater than that of dissolved O_2 at pH 2.0 for the reaction of $O_2 + 4H^+ + 4e^-$, whereas the H^+ concentrations (0.1–1.0 mmol L^{-1}) were lower than that of dissolved O_2 at pH 3.0–4.0 for the reaction. Experimental dependence of photocurrents on pH (Fig. 3B3) was consistent with kinetic model (equation 2) in the pH range between 2 and 4.

Experimental Methods. TiO_2 powder (1.00 g; P25, Degussa; anatase/rutile phases = 7/3; specific surface area 60 m^2 g^{-1}) was suspended in 3.0 mL of deionized water (< 0.06 μS cm^{-1}) and then stirred well. The suspension obtained was dried at 373 K for 24 h and heated in air at 673 K for 2 h. The resultant powder was suspended in 3.0 mL of deionized water and placed on ITO (thickness 1.2–1.6 μm)-coated Pyrex glass plate. The TiO_2/ITO/Pyrex was dried at 373 K for 18 h and heated in air at 573 K for 30 min. The amount of TiO_2 placed on ITO-coated glass was 5.0 mg, and the area covered was 1.3 cm^2.

Silver nitrate (17, 52, or 159 mg; 99.8%, Wako Pure Chemicals) was dissolved in 10 mL of deionized water. The solution was mixed with 3.33 g of untreated TiO_2 (P25). The mixture was magnetically stirred at a rate of 850 rpm and the water was distilled at 353 K. The obtained powder was dried at 373 K for 24 h and heated in air at 673 K for 2 h. The obtained Ag-TiO_2 powders contained 0.33, 1.0, and 3.0 wt% of Ag. They were suspended in minimum amount of water and placed on ITO-coated glass in a manner similar to that for the TiO_2/ITO/Pyrex.

TiO_2/ITO/Pyrex and Ag-TiO_2/ITO/Pyrex electrodes were immersed in HCl solutions (40 mL on each compartment; initial pH values between 2.0 and 4.0). The two compartments were separated by a 50 μm-thick PCP film (Nafion, Dupont; acid capacity > 9.2×10^{-4} equivalent g^{-1}). N_2 and O_2 gas were bubbled at 30 mm apart from each photoelectrode at a flow rate of 100 mL min^{-1} (Graphical abstract). The PFC was equipped with quartz windows (ϕ = 80 cm) on both sides. Both TiO_2 and Ag-TiO_2 photocatalysts were irradiated by UV-visible light through quartz windows via two-way branched quartz fiber light guide (5ϕ–2B–1000L, San-ei Electric Co.) from 500-W xenon arc lamp (Ushio, Model SX-UID502XAM). The distance between the light exit (ϕ = 5 mm) and TiO_2 or Ag-TiO_2 film was 46 mm. The

light intensity was 8 mW cm^{-2} at the center of the photocatalyst film on electrodes. The quantum efficiency of PFC was evaluated based on absorbed light (6.9%) by photocatalyst among incident light (1.7×10^{17} photons s^{-1}) to photocatalyst layers and short circuit current (74 μA ~ 4.6×10^{14} electrons s^{-1}; Fig. 3C). Overall efficiency of cell current per absorbed light was 0.04, and this can be considered as the product of efficiencies of anode (TiO_2) and cathode (Ag-TiO_2). If similar efficiency is assumed for electron generation at CB of anode and hole generation at VB of cathode, the product of 0.2×0.2 was 0.04.

Static photocurrent generation tests (Figs. 3A, B) were performed by connecting a external parallel circuit of a voltmeter, an ammeter, and a resistance of 0.5 Ω. A 30 min cycle of UV-visible light irradiation and 30 min of darkness was repeated on both photocatalysts, typically five times. The voltage between two electrodes and the current were monitored. The *i–V* dependence was also measured using a similar parallel circuit and the resistance was gradually decreased from 500 kΩ to 0.3 Ω over 20 min (Fig. 3C).

SEM, TEM, HR-TEM, and HAADF-STEM images were observed using TEM apparatus (Hitachi, Model HD2700 with an aberration-corrected STEM and an accelerating voltage of 200 kV. Cyclic voltammetry measurements were performed for Ag-TiO_2 (3.0 wt% of Ag) or TiO_2 as a working electrode (WE), glassy carbon as counter electrode, and Ag/AgCl as a reference electrode immersed in HCl solution of pH 4.0. The voltage of WE was swept between −1.0 and 1.0 V versus Ag/AgCl at the rate of 50 mV s^{-1} using a potentio/galvanostat (Model VersaSTAT 3-100, Princeton Applied Research) in O_2 or N_2 atmosphere at a flow rate of 100 mL min^{-1} under the irradiation by UV-visible light (8 mW cm^{-2}) or in dark.

Silver K-edge EXAFS spectra were measured at 290 K in transmission mode in the Photon Factory Advanced Ring at the High Energy Accelerator Research Organization (Tsukuba) on beamline NW10A. The storage ring energy was 6.5 GeV and the ring current was 537–355 mA. A Si (311) double-crystal monochromator and platinum-coated focusing cylindrical mirror were inserted into the X-ray beam path. The X-ray intensity was maintained at 65% of the maximum flux using a piezo translator set to the crystal. The slit opening size was 1 mm (vertical) × 2 mm (horizontal) in front of the ionization chamber. The silver K-edge absorption energy was calibrated to 25516.5 eV for the spectrum of Ag metal.[28] The

EXAFS data were analyzed using an XDAP package.[29] Multiple-shell curve-fit analyses were performed for the Fourier-filtered k^3-weighted EXAFS data in *k*- and *R*-space using empirical amplitude and phase-shift parameters extracted from the EXAFS data for Ag metal foil, Ag_2O, and AgCl powders. The interatomic distance (*R*) and its associated coordination number (*N*) for the Ag-Ag, Ag-O, and Ag-Cl pairs were set to 0.2889 nm with the *N* value of 12, 0.2044 nm with the *N* value of 2, and 0.2775 nm with the *N* value of 6 (Table S1).

References

(28) J. A.Bearden, *Rev. Mod. Phys.*, 1967, **29**, 78–124.

(29) M. Vaarkamp, H. Linders, and D. Koningsberger, *XDAP version 2.2.7*, XAFS Services International, Woudenberg, The Netherlands, 2006.

Table S1. The curve-fit analysis results of Ag K-edge EXAFS for Ag-TiO_2 (3.0 wt%-Ag) [a]

Sample		Ag-O	Ag-Cl	Ag-Ag	Goodness of fit
	R (nm)				
(a)		0.2305 (±0.0003)		0.287 (±0.002)	
673 K-calcined & under air (purple)	*N*	1.8 (±0.1)	—	2.0 (±0.1)	1.3×10^4
	$\Delta\sigma^2$ (10^{-5} nm^2)	7.6 (±0.3)		12 (±0.2)	
(b)		0.2038 (±0.0003)	0.262 (±0.001)	0.287 (±0.007)	
In *aq.* HCl (pH 2.0) & under N_2 (yellow)	*N*	0.9 (±0.2)	1.5 (±0.3)	1.5 (±0.1)	5.4×10^4
	$\Delta\sigma^2$ (10^{-5} nm^2)	−5.9 (±1.9)	−15 (±2.3)	3.7 (±2.8)	
(c)		0.2046 (±0.0005)		0.287 (±0.001)	
Under UV-visible (ocher)	*N*	0.3 (±0.1)	—	6.0 (±0.1)	1.6×10^5
	$\Delta\sigma^2$ (10^{-5} nm^2)	−7.3 (±3.5)		3.8 (±0.4)	
(d)		0.212 (±0.004)		0.284 (±0.004)	
Light off & under O_2 (purple)	*N*	1.5 (±0.1)	—	4.0 (±0.02)	2.3×10^5
	$\Delta\sigma^2$ (10^{-5} nm^2)	10 (±5.6)		8.5 (±0.4)	
(e)		0.2044	0.2775	0.2889	
Models (Ag_2O, AgCl, or Ag metal)	*N*	2	6	12	
	$\Delta\sigma^2$ (10^{-5} nm^2)	—	—	—	

[a] The values in parentheses are evaluated fit errors.

Table S2. Electrochemical data for Ag-TiO_2 (3.0 wt% of Ag)

Redox reaction Conditions	CV peak (V) Reduction wave	 Oxidation wave	 Center	Equil. voltage 298 K, pH 4.0
(A) $AgCl + e^- = Ag + Cl^-$				
O_2, Light	0.16	0.75	0.46	0.46
O_2, Dark	0.22	0.87	0.55	
N_2, Light	0.16	0.75	0.46	
N_2, Dark	0.22	0.87	0.55	
(B) $Ag_2O + 2H^+ + 2e^- = 2Ag + H_2O$				
O_2, Light	0.35	1.16	0.76	0.93
O_2, Dark	0.35	1.30	0.83	
N_2, Light	0.35	1.16	0.76	
N_2, Dark	—	—	—	
(C) $2H^+ + 2e^- = 2H_2$				
O_2, Light	—	—	—	−0.24
O_2, Dark	—	—	—	
N_2, Light	−0.25	—	—	
N_2, Dark	−0.26	—	—	
(D) $4H^+ + O_2 + 4e^- = 2H_2O$				0.99

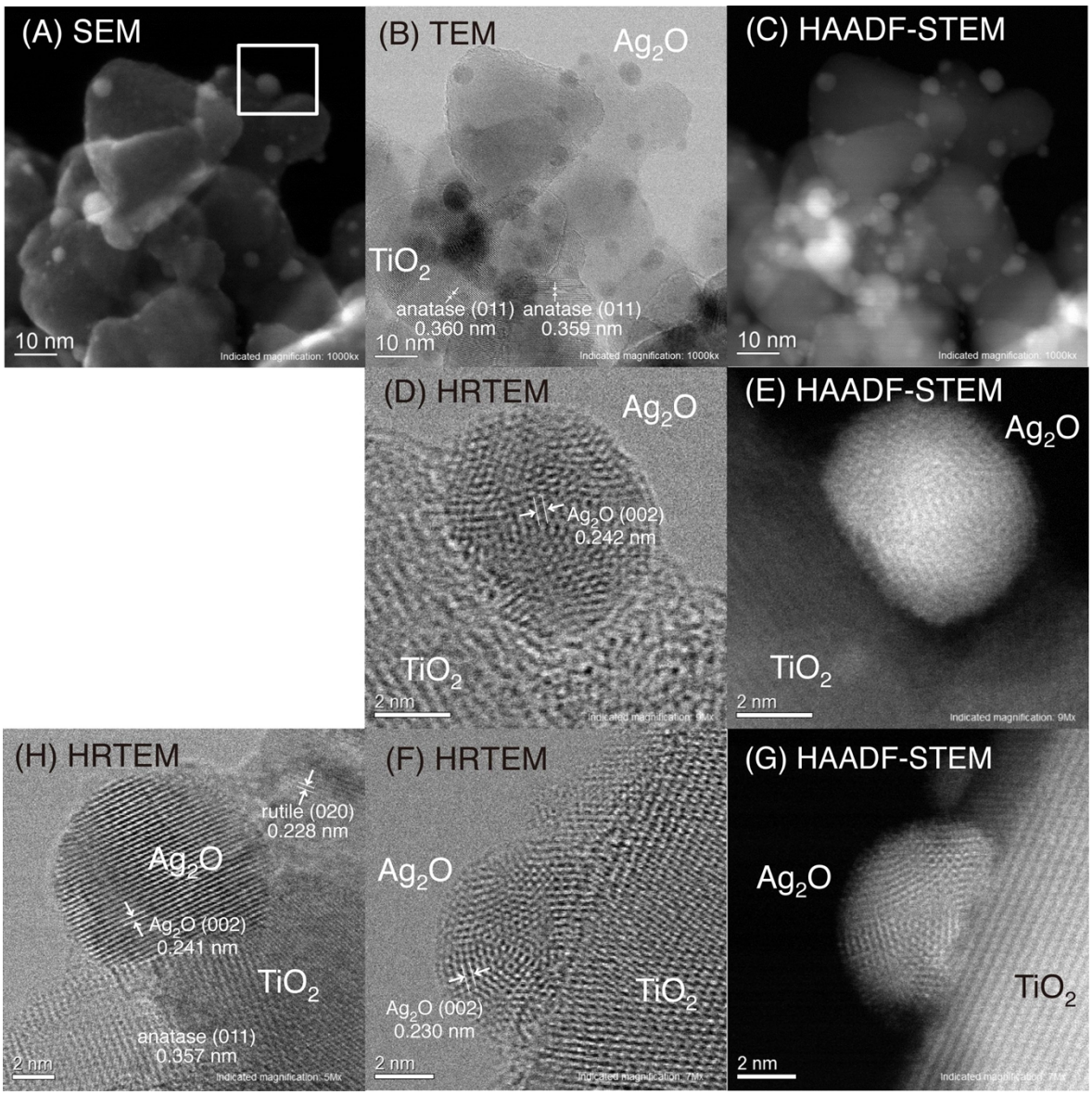

Fig. S1. SEM (A), TEM (B), HR-TEM (D, F, H), and HAADF-STEM images (C, E, G) measured for as-prepared Ag-TiO_2 photocatalyst stored in ambient air.